

The Tethered Moon

Kevin J. Zahnle^{a,*}, Roxana Lupu^b, Anthony Dobrovolskis^b, Norman H. Sleep^c

^a*Space Science Division, NASA Ames Research Center, MS 245-3, Moffett Field CA 94035 USA*

^b*SETI Institute, Mountain View CA 95064, USA*

^c*Department of Geophysics, Stanford University, Stanford CA 94305, USA*

Abstract

We address the thermal history of the Earth after the Moon-forming impact, taking tidal heating and thermal blanketing by the atmosphere into account. The atmosphere sets an upper bound of $\sim 100 \text{ W/m}^2$ on how quickly the Earth can cool. The liquid magma ocean cools over 2-10 Myrs, with longer times corresponding to high angular-momentum events. Tidal heating is focused mostly in mantle materials that are just beginning to freeze. The atmosphere's control over cooling sets up a negative feedback between viscosity-dependent tidal heating and temperature-dependent viscosity of the magma ocean. While the feedback holds, evolution of the Moon's orbit is limited by the modest radiative cooling rate of Earth's atmosphere. Orbital evolution is orders of magnitude slower than in conventional constant Q models, which promotes capture by resonances. The evection resonance is encountered early, when the Earth is molten. Capture by the evection resonance appears certain but unlikely to generate much eccentricity because it is encountered early when the Earth is molten and $Q_{\oplus} \gg Q_{\zeta}$. Tidal dissipation in the Earth becomes more efficient ($Q_{\oplus} \ll Q_{\zeta}$) later when the Moon is between $\sim 20R_{\oplus}$ and $\sim 40R_{\oplus}$. If lunar eccentricity grew great, this was when it did so, perhaps setting the table for some other process to leave its mark on the inclination of the Moon.

*Corresponding author

Email addresses: Kevin.J.Zahnle@NASA.gov (Kevin J. Zahnle), roxana.s.lupu@nasa.gov (Roxana Lupu), anthony.r.dobrovolskis@nasa.gov (Anthony Dobrovolskis), norm@stanford.edu (Norman H. Sleep)

Keywords:

Earth atmospheric evolution, Earth thermal evolution, Earth and Moon formation, Earth and Moon tidal evolution

Highlights

- We address the thermal history of the Earth after the Moon-forming impact.
- Thermal blanketing by Earth's atmosphere limits cooling to $\sim 100 \text{ W/m}^2$.
- Feedback between tidal heating and viscosity tethers the Moon to Earth.
- Slow orbital evolution promotes capture by resonances.
- Tidal Q's evolve differently in Earth and Moon

1. Introduction

The leading explanation for the origin of the Earth-Moon system is that it formed when two planets collided (Hartmann et al., 1986; Benz et al., 1986; Stevenson, 1987; Canup and Righter, 2000; Canup, 2004; Reufer et al., 2012; Čuk and Stewart, 2012; Canup, 2012). The event is widely known as the Moon-forming impact. But it might have been called the Earth-forming impact. Indeed, in some scenarios (e.g., Canup, 2012), neither of the two colliding planets is markedly more a proto-Earth than the other, in which case the Moon-forming impact is literally the Earth-forming impact as well.

Here we accept as an initial condition that a Moon-forming impact took place. We focus on the angular-momentum-conserving canonical model (Canup, 2004), although we also consider some aspects of recent non-angular-momentum-conserving alternatives (Reufer et al., 2012; Čuk and Stewart, 2012; Canup, 2012) that may better address isotopic evidence that the Earth and Moon share the same source (e.g., Pahlevan et al., 2007; Zhang et al., 2012).

Our subject here is the earliest thermal evolution of the Earth after the impact. Earth’s cooling was greatly slowed by the thermal blanketing effect of its atmosphere, which was thick and deep and very opaque, and Earth’s interior was strongly heated by tidal flexing, because the Moon was close by and the Earth was spinning rapidly. We stress here that tidal heating and thermal blanketing were linked, because radiative cooling by the atmosphere limits how big tidal heating can be. Hence we are also concerned here with the early tidal evolution of the Moon’s orbit, which we will treat as simply as possible. We first describe the thermal model of the cooling Earth in Section 2. We then describe tidal heating and tidal evolution in Section 3.

2. The cooling Earth

2.1. *Initial conditions*

A reasonable initial condition on the Earth after the Moon-forming impact is that it behaved like a hot liquid (Zahnle et al., 2006; Elkins-Tanton, 2008). The impact

itself melted and partially vaporized the side of the Earth that was directly struck. But even if half the mantle survived the shock of collision unmelted (Tonks and Melosh, 1993), it would have collapsed under its own weight on a Rayleigh-Taylor instability timescale of the order of

$$\tau \approx \frac{\rho\nu}{g \Delta\rho L}, \quad (1)$$

where L is the relevant length scale, g gravity, $\Delta\rho/\rho$ the density contrast between the solid and the melt, and ν the kinematic viscosity of the solid. For reasonable choices ($\Delta\rho/\rho = 0.02$, $L = 3 \times 10^8$ cm, $\nu = 10^{18}$ cm²/s, the latter appropriate to a warm silicate planet during accretion), the solid hemisphere would collapse in just 5 years and in the process releasing more than enough gravitational energy to melt what had not yet melted (Tonks and Melosh, 1993). Other factors — the impactor’s shock-heated molten iron plunging through the mantle to join with Earth’s core and the superheated state of the upper core immediately thereafter — also suggest that a liquid planet is a plausible initial condition.

It is important here to be careful defining what is meant by melting. Melting of a silicate is characterized by three temperatures: a liquidus T_{liq} hotter than which the silicate is fully molten; a solidus T_{sol} colder than which the silicate is fully solid; and a critical temperature T_{crit} in between at which the rheology of the material changes from that of a solid with melt percolating through it ($T < T_{\text{crit}}$) to a liquid carrying suspended solids (Abe, 1997; Solomatov, 2009). The critical temperature T_{crit} marks a phase transition in viscosity, which best corresponds to what is colloquially meant by a melting point. When the mantle collapses under its own weight, it is viscosity that converts that motion into heat. Viscous dissipation can only raise the temperature of the mantle to T_{crit} . To raise the temperature of such a lower mantle to the liquidus requires another mechanism, perhaps a prompt effect like the impactor’s shock-heated molten iron dispersing in the mantle before it joins with Earth’s core, or perhaps a delayed effect stemming from the mantle being strongly heated from below by the core.

Although very important to geochemistry, for our purposes it is not very important whether the mantle be fully or only partially molten, provided only that initially it behave like a low viscosity liquid. We therefore begin our study with a liquid mantle and a surface temperature of 3000-4000 K some 100-1000 years after the impact, by which point we can hope that early transients have settled down. On the other hand, these transients may last long enough to influence moon formation, which is also generally regarded as very fast (Canup, 2004; Salmon and Canup, 2012).

A second initial condition is the presence of a substantial atmosphere. Earth today has about 270 bars of H₂O and 50 bars of CO₂ near the surface, the former mostly in oceans and the latter mostly in carbonate rocks. Similarly large reservoirs are held in the mantle (Sleep et al., 2001). Thus it is reasonable to start with 100-1000 bars of H₂O and CO₂ in the atmosphere. The water vapor and carbon dioxide would be supplemented by smaller amounts of CO, H₂, N₂, various sulfur-containing gases, and by a suite of geochemical volatiles evaporated from the magma (Schaefer et al., 2012; Fegley and Schaefer, 2013).

A third initial condition is the existence of the Moon. We start the Moon with its current mass and density at the relevant Roche limit of $2.9R_{\oplus}$. Although accretion theory suggests that the Moon could accumulate in less than a year, the need to radiate the energy liberated by lunar accretion likely prolonged the process by decades or even centuries (Thompson and Stevenson, 1988; Ida et al., 1997; Genda and Abe, 2000; Canup, 2004; Salmon and Canup, 2012). During this time interactions between the accreting Moon and the unaccreted debris disk may raise the starting point of the Moon beyond the Roche limit to perhaps $\sim 5R_{\oplus}$ (Salmon and Canup, 2012). For our purposes starting the Moon nearer the Earth is more interesting because there is more tidal heating and more resonances to encounter as the Moon's orbit evolves.

A fourth initial condition is the initial angular momentum of the Earth-Moon system. In canonical models this is held constant, so that with the Moon forming at $2.9R_{\oplus}$, the Earth starts with a 5.0-hour day. Some recent Moon-forming models posit loss of angular momentum from the Earth-Moon system (Ćuk and Stewart,

2012; Canup, 2012). These begin the Earth with a ~ 3 -hour day, and thus with significantly more rotational energy available to be dissipated as tidal heating.

2.2. Interior Cooling

The total thermal energy E of the Earth is the sum of the thermal energy in the interior E_i and the thermal energy in the atmosphere E_{atm} . Our interest is almost entirely in the time rate of change of E ,

$$\dot{E} = -4\pi R_{\oplus}^2 \sigma T_{\text{eff}}^4 + \pi R_{\oplus}^2 F_{\odot} (1 - A) + \dot{E}_{\text{tide}}. \quad (2)$$

Equation 2 describes the Earth’s cooling rate as the difference between thermal infrared radiation emitted to space by the atmosphere and the sum of net insolation (radiative heating), tidal heating, and heating from the decay of radioactive elements. Thermal radiation (radiative cooling) to space is described by an effective radiating temperature T_{eff} , which is determined by the thermal blanketing effect of the atmosphere and the surface temperature T_s ; σ is the Stefan-Boltzmann constant and R_{\oplus} is the radius of the Earth. The relation between T_{eff} and T_s — the greenhouse effect — is discussed in the next section. Radiative heating is described by the solar constant $F_{\odot} \approx 1000 \text{ W m}^{-2}$ ca. 4.4 Ga and an albedo A . We leave $A = 0.3$ as today. Tidal heating \dot{E}_{tide} is a big term addressed in Section 3 below. With radioactive heating ignored, the geothermal heat flow F is equivalent to the rate of cooling of the interior,

$$4\pi R_{\oplus}^2 F = \dot{E}_{\text{tide}} - \dot{E}_i. \quad (3)$$

2.3. Radiative Cooling

It is well known that an atmosphere’s thermal blanketing effect prevents a magma ocean¹ from cooling rapidly. A string of increasingly sophisticated models, beginning with Matsui and Abe (1986) and proceeding through Abe and Matsui (1988); Zahnle

¹The term “magma ocean” is broadly used in the literature to describe a mantle with significant partial melt.

et al. (1988), Abe (1997), Zahnle et al. (2006), Elkins-Tanton (2008, 2012), Hamano et al. (2013), and Lebrun et al. (2013) have addressed some of the consequences of thermal blanketing by steam atmospheres over the Earth’s cooling magma oceans. Much of the progress made in these studies has been in constraining how the magma ocean freezes, how long it takes to freeze, and how, when, and what it degasses. All of these models presume H₂O-CO₂ atmospheres, and all but Zahnle et al. (2006) ignore the Moon.

A different set of studies has addressed the composition of the atmosphere (Schaefer and Fegley, 2010; Schaefer et al., 2012; Fegley and Schaefer, 2013; Lupu et al., 2014). Shortly after the impact the atmosphere over the lava is very hot and contains a great many geochemical volatiles that can evaporate from a magma ocean, such as sulfur, sodium, and chlorine, and many other compounds of H, C, N, and O in addition to H₂O and CO₂ (Schaefer et al., 2012; Fegley and Schaefer, 2013). The geochemically enriched atmosphere is more opaque than just H₂O and CO₂ at magma temperatures and thus the planet cools more slowly and spends more time with a lava surface than previous models would predict.

To address these issues we make use of new 1-D non-gray radiative-convective atmospheric structure models developed to compute the luminosity and spectral characteristics of Earth-like planets after giant impacts (Lupu et al., 2014). As the Lupu et al. (2014) models are discussed fully elsewhere we will not provide full documentation here, but we do note some key features. The new models include many of the molecular and atomic opacity sources that would be abundant in equilibrium with a hot rock or magma surface with the composition of the bulk silicate Earth (BSE, Lupu et al., 2014). The thermal structure models are computed as equilibrium models in which thermal radiation emitted by the atmosphere is balanced by the sum of sunlight absorbed and geothermal heat extracted from the cooling Earth. This assumption is very good because the heat capacity of the atmosphere is very small compared to the heat capacity of the planet. A more questionable assumption of the model is that it keeps the atmosphere in chemical equilibrium with the bulk

silicate Earth at any temperature — i.e., it assumes that CH_4 and NH_3 form when equilibrium chemistry would favor them. The assumption is reasonably good at high temperatures (at which CH_4 and NH_3 are rare in any case), but for temperatures much below 1000 K equilibrium would not be expected unless effective catalysts were present among the cloud particles. At low temperatures, equilibrium predicts that CH_4 and NH_3 would be present and effective as greenhouse gases, and thus the published Lupu et al. (2014) model may overestimate the greenhouse effect and underestimate T_{eff} when surface temperatures are below 500 K (above which H_2O is abundant). On the other hand, we are missing many opacity sources that would be present at higher temperatures, and thus in all likelihood the model underestimates the greenhouse effect when surface temperatures are above 1000 K. In practice we address the consequences of uncertain opacities by varying the total pressure of the atmosphere.

New calculations of T_{eff} for cloud-free runaway greenhouse H_2O - CO_2 - N_2 atmospheres (Goldblatt et al., 2013; Kopperapu et al., 2013) find that $T_{\text{eff}} = 265$ during the runaway greenhouse phase of planetary cooling. We expect that a deep CO_2 atmosphere will remain after the ocean of water condenses. This state was not addressed explicitly by Lupu et al. (2014). We therefore retrofitted a smooth transition to the ~ 500 K surface temperature expected under 100 bars of CO_2 (Zahnle et al., 2006). What happens to the CO_2 at later times on longer timescales is discussed elsewhere (Sleep et al., 2001, 2014).

2.4. Physical parameters

For present purposes a ruthlessly simplified model of the Earth is the best choice. We characterize the Earth by a surface temperature T_s and an interior temperature T_i . In effect T_i is the potential temperature, the temperature that every parcel in an adiabatic mantle would have were it brought to the surface. We also assume that the mantle is uniform, in the sense that it has the same viscosity at all depths and that it freezes everywhere at the same time. This assumption is roughly equivalent to assuming that the adiabat and the melting curve are parallel. We take $T_{\text{liq}} = 1800$

K and $T_{\text{sol}} = 1400$ K. These are arbitrary values; our results are insensitive to them. We assume that the melt fraction ϕ is linear in T_i between T_{liq} and T_{sol} ,

$$\begin{aligned} \phi &= 1 & T_i &> T_{\text{liq}} \\ \phi &= (T_i - T_{\text{sol}}) / (T_{\text{liq}} - T_{\text{sol}}) & T_{\text{liq}} &> T_i > T_{\text{sol}} \\ \phi &= 0 & T_{\text{sol}} &> T_i. \end{aligned} \quad (4)$$

For $T_i > T_{\text{liq}}$ and $T_i < T_{\text{sol}}$, the heat capacity of the Earth is

$$C_{v\oplus}M_{\oplus} = C_{v,\text{man}}M_{\text{man}} + C_{v,\text{cor}}M_{\text{cor}} = 6.2 \times 10^{30} \text{ J/kg/K}, \quad (5)$$

in which the masses of the Earth, the mantle, and the core are M_{\oplus} , M_{man} and M_{cor} , respectively. The heat capacity of silicate is approximated by $C_{v,\text{man}} = 1200$ J/kg/K and that of iron by $C_{v,\text{cor}} = 650$ J/kg/K. The iron core does not freeze on the time scale of interest. While silicates freeze, the effective heat capacity of the Earth is

$$C'_{v\oplus}M_{\oplus} = C_{v\oplus}M_{\oplus} + \frac{Q_m M_{\text{man}}}{T_{\text{liq}} - T_{\text{sol}}} = 1.0 \times 10^{31} \text{ J/kg/K} \quad (6)$$

where the heat of fusion is $Q_m = 4 \times 10^5$ J/kg. With the above simplifications, the relation between \dot{E}_i and \dot{T}_i is

$$\begin{aligned} \dot{E}_i &= C_{v\oplus}M_{\oplus}\dot{T}_i & T_i &> T_{\text{liq}}, T_{\text{sol}} > T_i \\ \dot{E}_i &= C'_{v\oplus}M_{\oplus}\dot{T}_i & T_{\text{liq}} &> T_i > T_{\text{sol}}. \end{aligned} \quad (7)$$

Including the atmosphere, the total \dot{E} is

$$\dot{E} = \dot{E}_i + C_{v,\text{atm}}M_{\text{atm}}\dot{T}_s, \quad (8)$$

in which \dot{T}_s is related to \dot{T}_i by the equations of parameterized convection described in the next section. The thermal energy in the atmosphere is a small term.

2.5. Parameterized convection

We follow previous workers by using parameterized convection to link the cooling rate to the temperature and heat generation inside the Earth (Solomatov, 2009;

Lebrun et al., 2013). In parameterized convection, the geothermal heat flow F

$$F = C_0 \frac{k_c (T_i - T_s)}{L} Ra^n \quad (9)$$

is related to the size and viscosity of the interior and the temperature gradient across the surface boundary layer through the Rayleigh number Ra ,

$$Ra = \frac{\alpha_v g (T_i - T_s) L^3}{\kappa \nu}. \quad (10)$$

Equations 9 and 10 can be combined to give a closed-form expression for $F(T_s, T_i)$,

$$F = C_0 k_c (T_i - T_s)^{1+n} L^{3n-1} \left(\frac{\alpha_v g}{\kappa \nu(T_i)} \right)^n. \quad (11)$$

We use $k_c = 500 \text{ J/m}^2/\text{s/K}$ for the thermal conductivity; α_v is the volume thermal expansivity, g the gravity, and κ is the thermal diffusivity ($\kappa \equiv k_c/C_{v,\text{man}}/\rho$). We will use $\alpha_v = 2.4 \times 10^{-5} \text{ K}^{-1}$, $\kappa = 10^{-6} \text{ m}^2/\text{s}$, and $g = 10 \text{ m/s}^2$. The characteristic distance scale L is usually identified with the thickness of the mantle. In the soft turbulent regime we take $C_0 = 0.089$ and $n = 1/3$ (Solomatov, 2009). With $n = 1/3$, L cancels out, so that the heat flow is determined only by the properties of the boundary layer.

The kinematic viscosity ν (m^2/s) is a very strong function of temperature T_i and therefore of central importance to convection and tidal heating. We follow Abe (1997); Solomatov (2009); Lebrun et al. (2013) by treating the temperature dependence of viscosity in two regimes, the hotter resembling a liquid and the cooler resembling a solid, the regimes divided by T_{crit} . The phase transition is a sharp function of the fraction ϕ of silicate that is liquid. In the liquid, Solomatov (2009) parameterizes viscosity by

$$\nu(T_i > T_{\text{crit}}) = 6 \times 10^{-8} \exp\left(\frac{4600 \text{ K}}{T_i - 1000 \text{ K}}\right) \left(\frac{1 - \phi_{\text{crit}}}{\phi - \phi_{\text{crit}}}\right)^{2.5} \text{ m}^2/\text{s}. \quad (12)$$

This expression implies that $\nu \rightarrow \infty$ as $\phi \rightarrow \phi_{\text{crit}}$; i.e., it is singular at $\phi = \phi_{\text{crit}}$. In the solid,

$$\nu(T_i < T_{\text{crit}}) = 1 \times 10^{15} \exp\left(\frac{T_{\text{sol}} - T_i}{58 \text{ K}}\right) \exp(-\alpha_\phi \phi) \text{ m}^2/\text{s}, \quad (13)$$

with $\alpha_\phi = 26$ (Solomatov, 2009). Abe (1997) places the boundary at $\phi = \phi_{\text{crit}} = 0.4$. For $\phi_{\text{crit}} = 0.4$, $T_{\text{crit}} = 1560$ K. The particular values of ϕ_{crit} and T_{crit} are unimportant. Figure 1 illustrates the situation.

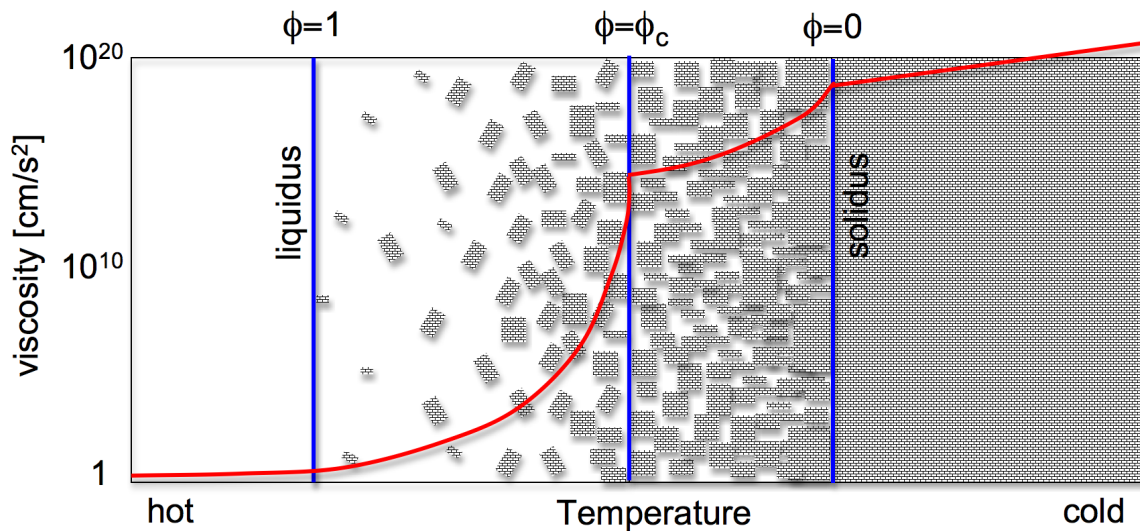


Figure 1: Semi-quantitative cartoon illustrating the rheological transition in a cooling magma ocean. Cooling proceeds from left to right. At the liquidus refractory crystals begin to freeze out. With further cooling the crystal fraction increases and the liquid fraction ϕ decreases. At the rheological transition $\phi = \phi_c \approx 0.4$. At the solidus the melt fraction $\phi = 0$. The corresponding kinematic viscosity ν is shown on a logarithmic scale. The discontinuity in ν at $\phi = \phi_c$ ($T_i = T_{\text{crit}}$) corresponds to a melting point.

2.6. Moonless Earths

Impacts on the scale of the Moon-forming impact need not create a moon. It is illustrative to consider a case without the Moon for comparison with previous work (Hamano et al., 2013; Lebrun et al., 2013). Computed temperatures and heat flow histories for a 100 bar BSE-equilibrated atmosphere are shown in Figure 2. In these simulations the initial temperature is set at $T_i = 3500$ K at $t = 100$ years.

Cooling takes place in two sharply defined regimes (Figure 2). In the first regime

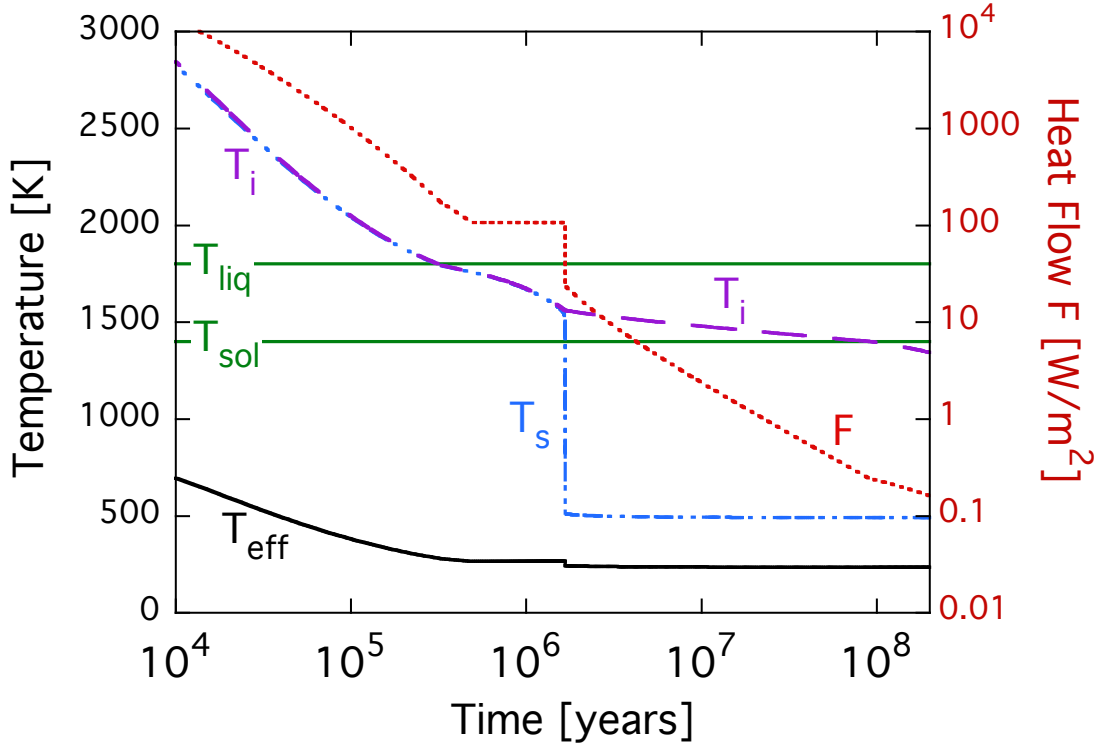


Figure 2: Thermal evolution of an Earth after a non-moon-forming giant impact of the same energy as the canonical Moon-forming impact. Results are shown for a 100 bar BSE atmosphere. Internal temperature T_i (mantle), surface temperature T_s , and effective radiating temperature T_{eff} are plotted against the left-hand axis. The liquidus and solidus are indicated. Geothermal heat flow F (dotted curve) is plotted against the right-hand axis. The heat flow plateaus at $F \sim 110$ W/m^2 while the Earth passes through the runaway greenhouse, a phase that lasts from ~ 0.5 Myr to ~ 1.7 Myr. This period corresponds to a liquid mantle. It ends when the mantle becomes too viscous to sustain $F \sim 110$ W/m^2 , at which point T_s drops to low values, here ~ 500 K under ~ 100 bars of CO_2 . The mantle remains partially molten for ~ 100 Myrs. The latter is what is often meant by “magma ocean.”

the three leading terms in the planet’s energy budget,

$$\sigma T_{\text{eff}}^4 = (1 - A) F_{\odot}/4 + F, \quad (14)$$

are of comparable magnitude, with the geothermal heat flow $F \sim 110$ W/m^2 making

up the difference between net insolation $\sim 170 \text{ W/m}^2$ and radiative cooling at the runaway greenhouse threshold $\sim 280 \text{ W/m}^2$. In this regime the temperature contrast $\Delta T = T_i - T_s$ across the surface thermal boundary layer is small compared to T_i . This lasts about 1 million years. The transition to the second regime takes place when the mantle’s viscosity grows too great to sustain $F \sim 110 \text{ W/m}^2$, at which point the mantle undergoes the phase transition depicted in Figure 1. After the phase transition heat flow is negligible (here $\sim 20 \text{ W/m}^2$ at first, but falling off fairly quickly) and the surface temperature is determined by insolation and the greenhouse effect of ~ 100 bars of CO_2 .

As Matsui and Abe (1986) and Hamano et al. (2013) point out, the value $F \approx 110 \text{ W/m}^2$ is particular to ancient Earth with insolation $F_\odot = 1.0 \times 10^3 \text{ W/m}^2$ and albedo $A = 0.3$. At Venus’s distance from the Sun, the heat flow required to support a runaway greenhouse atmosphere with $A = 0.4 \pm 0.1$ is of the order of $F = 10 \pm 40 \text{ W/m}^2$. Venus after the impact could have been held in a state with a molten surface for tens of millions of years or more, and if its albedo were less than $A \approx 0.38$ it need not have emerged from this state until after its water was lost to space (Hamano et al., 2013).

3. The Moon and Tides

Tidal heating by the nearby Moon was a major term in early Earth’s energy budget. The heat comes from braking the rotation of the Earth. Tidal dissipation is usually described by the Q parameter, defined as the fraction of energy in the wave that is damped out during a single period (Goldreich and Soter, 1966). The value of Q can often be deduced empirically while presupposing nothing about the underlying physics of tidal dissipation. We will use Q , but for the congealing mantle we will assume that tidal dissipation can be described by viscosity. This is a reasonable approximation as the mantle starts to freeze because ordinary viscous dissipation would be big (Moore, 2003). Where viscous dissipation dominates, Q can be computed (i.e., instead of assuming Q directly, we assume a particular physi-

cal mechanism for dissipation and a particular description of how viscosity evolves). But at very early times when the mantle is effectively inviscid, or at modern times when the mantle is solid, ordinary viscous dissipation is probably negligible and some other source of dissipation will likely be more important. In a hot molten Earth we use observed values of Q in fluid planets as a guide. For modern times we assume an asymptotic viscosity that brings the Earth-Moon system to its current state in 4.5 Ga, it being understood that the bulk of tidal dissipation on the Earth today actually takes place at the interface between the solid surface and the liquid water oceans (Lambeck, 1980).

3.1. Simple tidal dissipation

We assume that, locally, viscous tidal dissipation scales as the viscosity multiplied by the square of the strain rate $\dot{\epsilon}$. The strain ϵ is the fractional (dimensionless) deformation induced by the tide. It is of order of H/R_{\oplus} , where H is the amplitude of the tide. The rate of strain is therefore on the order of $\dot{\epsilon} = Hf/R_{\oplus}$, where f is the forcing frequency of the tide. Viscous heating per unit volume scales as $\rho\nu\dot{\epsilon}^2$, which for a uniform planet equates to $M_{\oplus}\nu\dot{\epsilon}^2$ as a whole. The peak-to-peak amplitude of the lunar semidiurnal equilibrium tide is

$$H = \frac{3}{2}h_2R_{\oplus}\left(\frac{M_{\zeta}}{M_{\oplus}}\right)\left(\frac{R_{\oplus}}{a}\right)^3, \quad (15)$$

in which M_{ζ} is the mass of the Moon, a is the semimajor axis of the Moon's orbit, and h_2 is the amplitude Love number (Kaula, 1968),

$$h_2 = \frac{5}{2}\left(1 + \frac{19}{2}\frac{\mu}{\rho g R_{\oplus}}\right)^{-1}. \quad (16)$$

The dimensionless quantity $(19/2)(\mu/\rho g R_{\oplus})$ compares the material rigidity μ (resistance to shear) to the weight of the Earth. The angular frequency of the semidiurnal lunar tide — the only tide we will consider here — is $f = 2\Omega - 2n_1$, where n_1 denotes the angular velocity of the Moon in its orbit.

Viscous heating must be modified to take into account how quickly matter can respond to forcing. The resulting heuristic expression² for tidal dissipation in Earth is

$$\dot{E}_{\text{tide}} \approx \frac{M_{\oplus} \nu \dot{\epsilon}^2}{1 + f^2 \tau_{\nu}^2}, \quad (17)$$

where τ_{ν} represents the viscous relaxation time scale, which is best written (M. Efroimsky, personal communication) in the form

$$\tau_{\nu} = \tau_{\text{M}} + \tau_{\text{D}} \quad (18)$$

with $\tau_{\text{M}} \equiv \rho\nu/\mu$ being the Maxwell time scale and $\tau_{\text{D}} \equiv 19\nu/2gR_{\oplus}$ being Darwin's time scale for relaxation of a viscous globe under its own gravity (Lamb, 1932, p. 641). Expressions in the form of Eq. 17 are often encountered in the planetary literature to describe tidal dissipation in a variety of objects (e.g., Moore, 2003; Garrick-Bethell et al., 2010). For the shear modulus μ we assume

$$\begin{aligned} \mu &= 0 & T_i &> T_{\text{crit}} \\ \mu &= 1.3 \times 10^{11} \exp(-\alpha_{\phi}\phi) & T_{\text{crit}} &> T_i > T_{\text{sol}} \\ \mu &= 1.3 \times 10^{11} & T_{\text{sol}} &> T_i \end{aligned} \quad (19)$$

where the units of μ are kg/m/s. The shear modulus is related to the Love numbers h_2 (Eq 16) and k_2 (Eq 23). For Earth today, Kaula (1968) and Lambeck (1980) give $h_2 \approx 0.6$ and $k_2 \approx 0.3$. These values imply that $\mu = 1.3 \times 10^{11}$ kg/m/s can be used as an effective average rigidity of the Earth today. The presumed temperature dependence of μ in Eq. 19 is arbitrary.

Viscous dissipation can be expressed in terms of Q . Kaula (1968, Eq. 2.3.1) defines Q as

$$\frac{2\pi}{Q} \equiv \frac{1}{E} \oint \dot{E} dt \quad (20)$$

²According to Makarov and Efroimsky (2014), this is exact if multiplied by a factor of 19/25.

where E represents the energy in the wave and the integral is over one full cycle. This is equivalent to writing

$$Q = \dot{E}_{\text{pot}}/\dot{E}_{\text{tide}}, \quad (21)$$

where the total potential energy in the tidal wave is (Kaula, 1968, p. 201).

$$\dot{E}_{\text{pot}} = \frac{3}{4}k_2GM_{\text{C}}^2 \frac{R_{\oplus}^5}{a^6} f, \quad (22)$$

where the potential Love number is

$$k_2 = \frac{3}{2} \left(1 + \frac{19}{2} \frac{\mu}{\rho g R_{\oplus}} \right)^{-1}. \quad (23)$$

We use Eq. 21 to generate Q_{\oplus} .

At temperatures below the solidus, for which viscosity is very large, ordinary viscous dissipation at tidal frequencies is probably unimportant. To bring the Moon to its present orbit at the present time requires $Q_{\oplus} \sim 30$, which we obtain by setting an upper bound on “viscosity” in Eq. 17 of $\nu_{\text{max}} = 1.3 \times 10^{13} \text{ m}^2/\text{s}$. We apply the upper bound on ν only to tidal dissipation in Eq 17. We do not apply it to the Rayleigh number and related quantities pertinent to parameterized convection.

At high temperatures the ordinary viscosity of mantle liquids is expected to be very small. With $\nu = 10^{-4} \text{ m}^2/\text{s}$, we estimate that $Q_{\oplus} \sim \sigma_2 \tau_2 \sim 10^{14}$, where $\sigma_2 = 4g/5R_{\oplus}$ is the relevant natural oscillation frequency of a self-gravitating fluid globe (Lamb, 1932, art. 262, Eq. 10) and $\tau_2 = R_{\oplus}^2/5\nu$ is the relevant timescale for viscous dissipation in a self-gravitating fluid globe when viscosity is small (Lamb, 1932, art. 355, Eq. 12). Convecting fluid planets may provide useful guidance. General constraints set by tidal evolution of the Galilean satellites suggest that Q of Jupiter is between 10^5 and 10^6 (Goldreich and Soter, 1966). Astrometric observations suggest that Q of Jupiter is $\sim 3.5 \times 10^4$ (Lainey et al., 2009) and Q of Saturn just 1400 (Lainey et al., 2012), the latter remarkably low compared to the 7×10^4 estimated by Goldreich and Soter (1966). The uncertainty and variance reminds us that origin of dissipation in the giant planets is unknown. Similar arguments have been made for binary stars; these suggest that Q is of the order of $10^5 - 10^6$ (Meibom and

Mathieu, 2005). On the other hand, at least one hot superJupiter—the 10 Jupiter mass WASP-18b, currently parked in a 0.94 day orbit—may require $Q > 10^9$ (Hellier et al., 2009).

3.2. Simple tidal evolution

The simplest assumption is that the Moon evolved away from the Earth while maintaining a circular orbit. We will make this assumption here. The Moon revolves about the Earth at the angular frequency

$$n_1 = \sqrt{G(M_{\oplus} + M_{\zeta})/a^3}. \quad (24)$$

The total Earth-Moon system angular momentum ignoring lunar spin and assuming a circular orbit is

$$L = I_{\oplus}\Omega + M_{\zeta} \sqrt{G(M_{\oplus} + M_{\zeta})} a, \quad (25)$$

in which Ω denotes Earth’s angular rotation rate. The canonical model of the Moon-forming impact assumes that the angular momentum of the Earth-Moon system has been conserved. With $\dot{L} = 0$, the Moon recedes at the rate

$$\dot{a} = \frac{-2I_{\oplus}\dot{\Omega}a}{L - I_{\oplus}\Omega}. \quad (26)$$

With \dot{a} given by Eq 26, the tidal dissipation is related to the rate of braking of Earth’s spin by

$$\dot{E}_{\text{tide}} = - \left(I_{\oplus}\Omega - \frac{GM_{\oplus}M_{\zeta}}{a} \frac{I_{\oplus}}{L - I_{\oplus}\Omega} \right) \dot{\Omega}, \quad (27)$$

in which $I_{\oplus} = 0.33 M_{\oplus} R_{\oplus}^2$ represents Earth’s moment of inertia. Note that $\dot{\Omega}$ is negative and \dot{a} and \dot{E}_{tide} are positive.

Figure 3 shows thermal evolution of an Earth after a canonical Moon-forming impact that forms a Moon. Other particulars are the same as with the moonless impact of Figure 2. Tidal heating extends the duration of the runaway greenhouse phase by a few hundred thousand years, and greatly increases geothermal heat flow for tens of millions of years afterward, but at first glance the differences between Figures 2 and 3 are subtle.

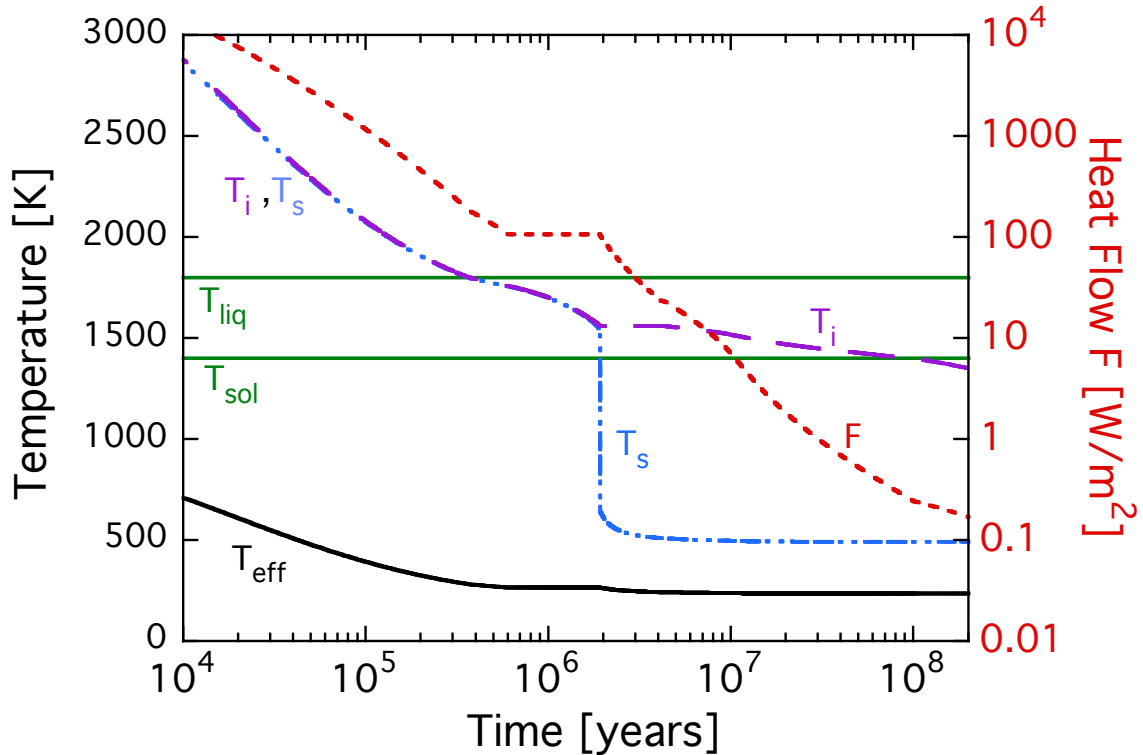


Figure 3: Thermal evolution of the Earth after a canonical Moon-forming impact. Results are shown for the 100 bar BSE-equilibrated atmosphere. The results are very similar to Figure 2. Tidal heating extends the runaway greenhouse phase by a few hundred thousand years compared to the moonless case. Geothermal heat flow F is about an order of magnitude higher than in the moonless case for a few tens of Myrs.

Changing the radiative properties of the atmosphere has greater effect than adding the Moon. Figure 4 shows a comparable thermal evolution under a 1000 bar post-impact atmosphere. This is toward the thicker end of the range we might expect for Earth, but the thicker atmosphere also serves as a proxy for additional opacity sources that are undoubtedly present at very high temperatures but are not included in our model, or a proxy for the greater opacity of an atmosphere that is more reduced than the BSE. The thicker atmosphere increases how long Earth remains liquid by an order of magnitude, from ~ 0.3 Myrs for the 100 bar atmosphere

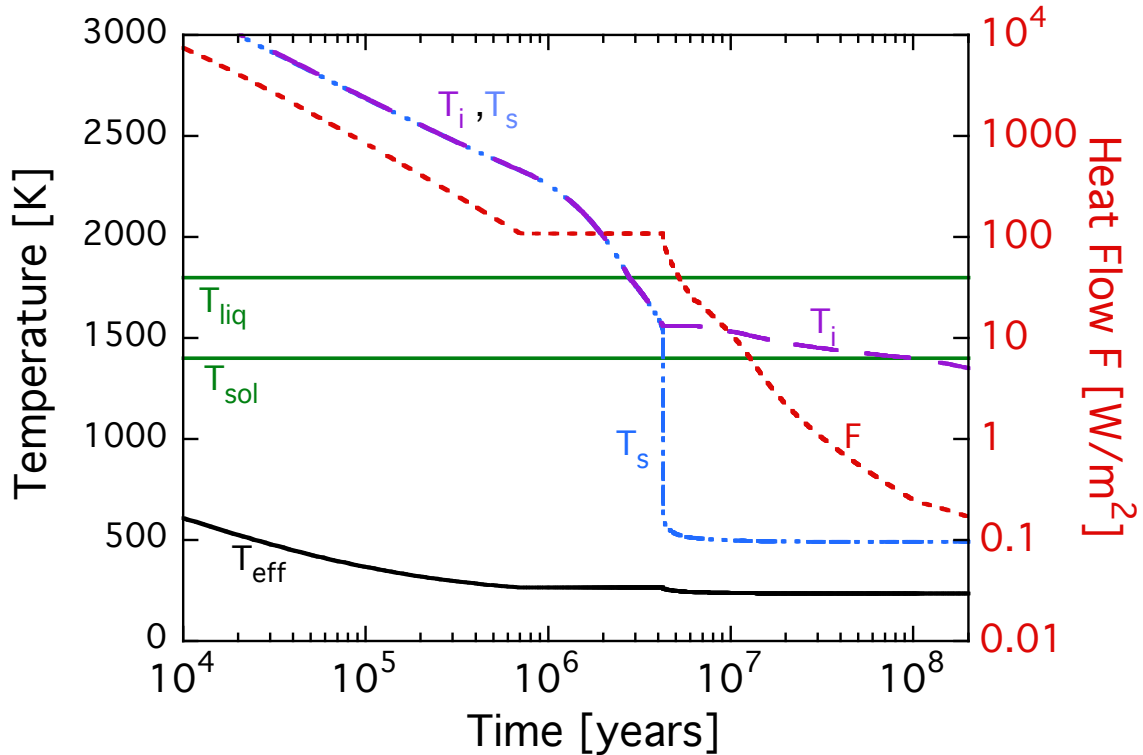


Figure 4: Thermal evolution of the Earth after a canonical Moon-forming impact, with more volatiles. Results are shown for a 1000 bar BSE-equilibrated atmosphere. The thicker atmosphere more than doubles the duration of the runaway greenhouse phase, and increases the Earth’s fully molten stage from 0.3 Myrs (Fig. 3) to 3 Myrs.

to ~ 3 Myrs. The thicker atmosphere also doubles how long the Earth remains in the runaway greenhouse state (from ~ 2 to ~ 4 Myr). Since the two cases start with the same amount of thermal and rotational energy, the differences between Figures 3 and 4 stem from how quickly the atmosphere radiates when it is much hotter than the runaway greenhouse state. This in turn is determined by the opacity of the atmosphere when the surface is very hot, $T_s > 2500$ K, a kind of atmosphere that is only now beginning to be studied.

It is interesting to consider what these models predict for the evolution of the distance to the Moon and the parameter Q_{\oplus} of the Earth. Figure 5 shows two cases

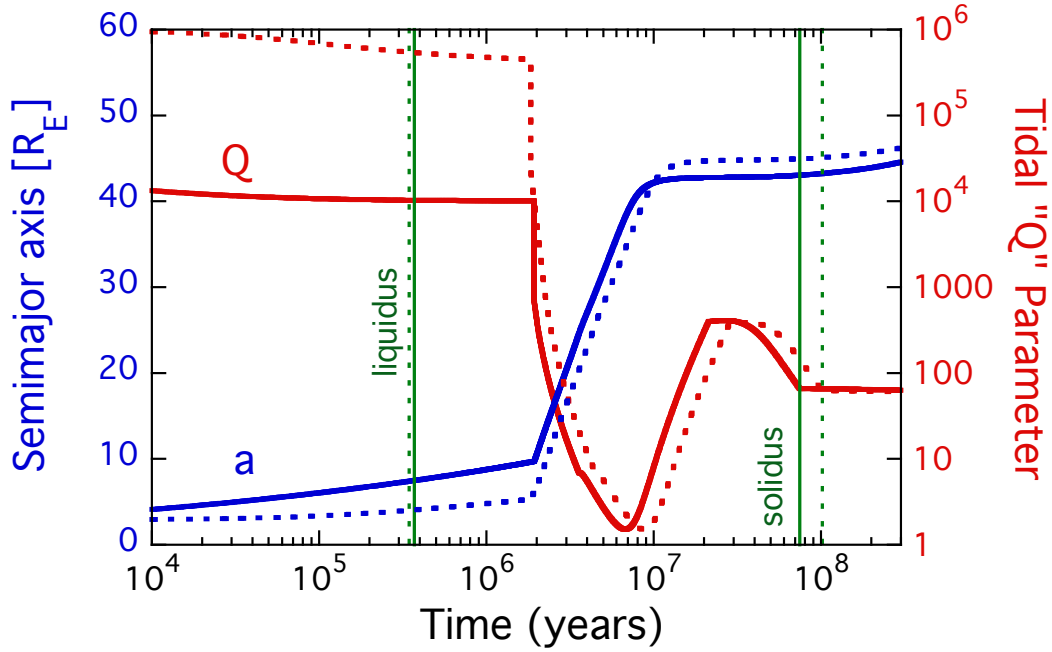


Figure 5: The distance to the Moon a and the tidal dissipation parameter Q_{\oplus} of the Earth after a canonical Moon-forming impact. Results are shown for high (dotted) and low (solid) values of Q in the fully molten Earth. As it congeals, the mantle becomes extremely dissipative with Q_{\oplus} near unity and the Moon’s orbit evolves quickly. After the mantle freezes the viscosity increases, Q_{\oplus} increases, and the Moon settles down. Both models assume a relatively thin 100 bar BSE-equilibrated atmosphere. The 1000 bar atmosphere gives qualitatively similar results.

that differ only in the assumed upper bound on $10^4 < Q_{\oplus} < 10^6$ for the fully liquid Earth. Both cases assume the Earth is enveloped in the 100 bar atmosphere. There are no striking differences between the two models. A minor difference is that the higher Q_{\oplus} model delays tidal heating somewhat, thus extending the lifetime of the magma ocean (defined as $T_i > T_{\text{sol}}$) from 70 to 100 Myrs. The 1000 bar atmosphere gives qualitatively similar results, with a somewhat slower tidal evolution and a somewhat longer-lived magma ocean.

3.3. The Evection and Eviction Resonances

The evection resonance describes the state in which the perigee of the Moon’s orbit precesses in one year (Touma and Wisdom, 1998). While the Moon is in the evection resonance, its line of apsides remains nearly at a constant angle to the Sun, and thus the Sun’s gravitational torque on the Earth-Moon system does not average out, but rather becomes cumulative. This enables transfer of angular momentum from the Earth-Moon system to the Earth’s orbit about the Sun (Ćuk and Stewart, 2012).

The possible importance of the evection resonance to the history to the lunar orbit was pointed out by Touma and Wisdom (1998). They showed that, if the Earth-Moon angular momentum were conserved, the evection resonance would have been encountered at $a \approx 4.6R_{\oplus}$, and that capture by the resonance from a nearly circular orbit is likely if $da/dt < 1$ km/yr, but unlikely if $da/dt > 10$ km/yr. They compared these results to a conventional constant Q model that predicts $da/dt \approx 150$ km/yr at $a \approx 4.6R_{\oplus}$. Touma and Wisdom (1998) found that if captured the Moon can evolve into a highly eccentric orbit with $e \approx 0.5$, which in their model is what allows the Moon to escape the resonance.

Integrations of the lunar orbit backward in time indicate that today’s 5° inclination to the ecliptic maps to a $\sim 10^{\circ}$ inclination with respect to Earth’s equator when the Moon was near the Earth (Goldreich, 1966; Mignard, 1980). In the giant impact hypothesis, the Moon should have formed in Earth’s equator and hence should have no inclination today. Ward and Canup (2000) proposed that a resonant interaction between the nascent Moon and the debris disk interior to it could generate an inclination of the right magnitude. Touma and Wisdom (1998) suggested that tidal evolution could raise the Moon’s inclination if the Moon were captured successively, first by the evection resonance, and then by a closely related “eviction” resonance. The evection resonance gives the lunar orbit substantial eccentricity. The eviction resonance can then give it substantial inclination. The chief challenge is that, to be captured by the eviction resonance, the Moon must be evolving inward at the

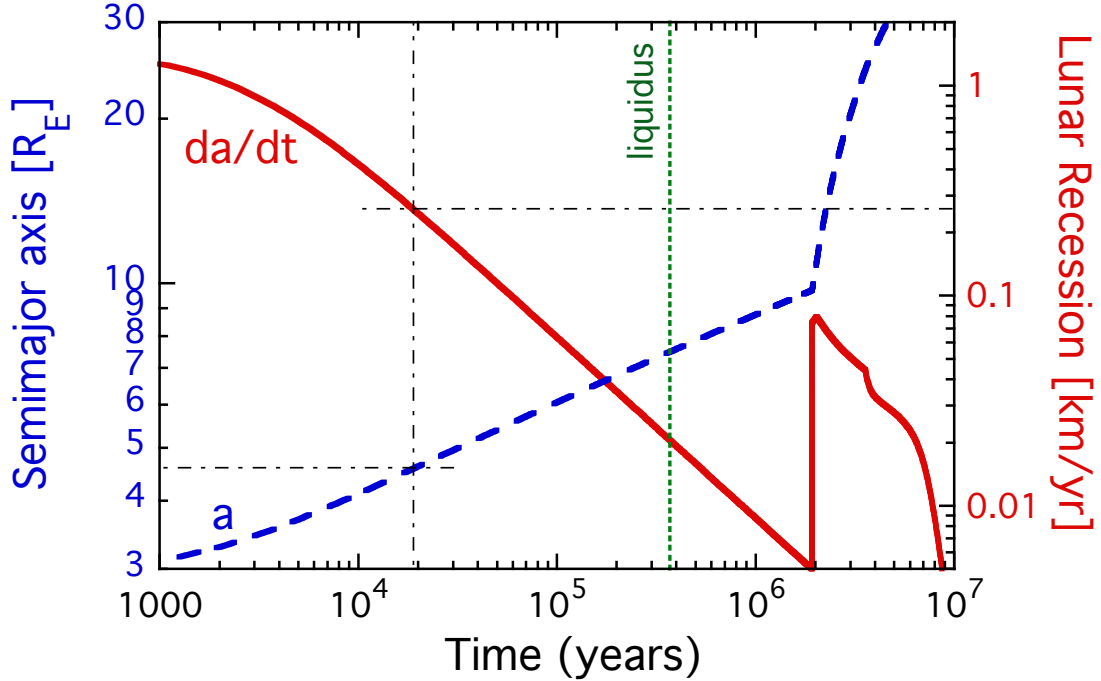


Figure 6: Distance to the Moon a and lunar recession rate da/dt are plotted for our standard case with a 100 bar BSE atmosphere. Touma and Wisdom (1998) show that the evection resonance is encountered at $a \sim 4.6R_{\oplus}$, and that resonance capture from a near circular orbit requires $da/dt \leq 1$ km/yr. The dot-dashed lines indicate that the resonance at $4.6R_{\oplus}$ is met early, after just 20,000 Myrs (before the mantle has cooled to the liquidus), and that $da/dt < 0.3$ km/yr, the latter making resonance capture very probable.

time ($\dot{a} < 0$), possible only if the Moon were in a very eccentric orbit. They find by numerical experiment that capture by the evicton resonance requires $|da/dt| < 0.2$ km/yr.

Figure 6 illustrates that thermal blanketing by Earth’s atmosphere slows early tidal evolution of the Earth-Moon system by orders of magnitude compared to $da/dt = 150$ km/yr. The slow rate of tidal evolution makes resonance capture seem likely. But we do not see much hope for the evicton mechanism here. The problem is that the resonance encounters occur very early, when the Earth is still effectively inviscid, but not so early that the airless Moon is likely to be fully molten. With

tidal dissipation efficient in the Moon but inefficient in the Earth, the Moon's orbit cannot acquire the substantial eccentricity that it would need to be captured by eviction. We expect rather that the Moon does not acquire a substantial eccentricity until the Earth begins to freeze and Q_{\oplus} becomes small, which becomes the case when $20R_{\oplus} < a < 40R_{\oplus}$.

3.4. New Conventions

Recently, Čuk and Stewart (2012) showed that, if the Earth-Moon system began with more angular momentum than it has today, the evection resonance occurs further from the Earth (because the faster spinning Earth is more oblate), which makes resonance capture more probable. In their model the resonance remains occupied during a second contraction phase where both e and a slowly decrease. They also showed that, if the Earth-Moon system began with more angular momentum than it has today, it would lose that angular momentum while captured in the evection resonance.

To approximate the evection mechanism at a level appropriate for this study, we assume that when the Moon encounters the resonance at distance a_r , it remains trapped while $L > L_{\text{now}}$. Following Touma and Wisdom (1998), we approximate the location of the evection resonance by

$$\left(\frac{a_r}{R_{\oplus}}\right)^{7/2} = \frac{3}{2} J_2 \frac{n_1}{n_2}, \quad (28)$$

in which n_1 (Eq. 24) and n_2 are the angular velocities of the month and year, and

$$J_2 = J_{20} \left(\frac{\Omega}{\Omega_o}\right)^2 \quad (29)$$

approximates the oblateness of the Earth with $J_{20} = 0.00108$. With these assumptions,

$$\dot{E}_{\text{tide}} = -I_{\oplus} \Omega \dot{\Omega} - \frac{1}{2} M_{\zeta} n_1^2 a_r \dot{a}_r \quad (30)$$

and the angular momentum of the Earth-Moon system decreases as

$$\dot{L} = I_{\oplus} \dot{\Omega} + M_{\zeta} n_1 a_r \dot{a}_r. \quad (31)$$

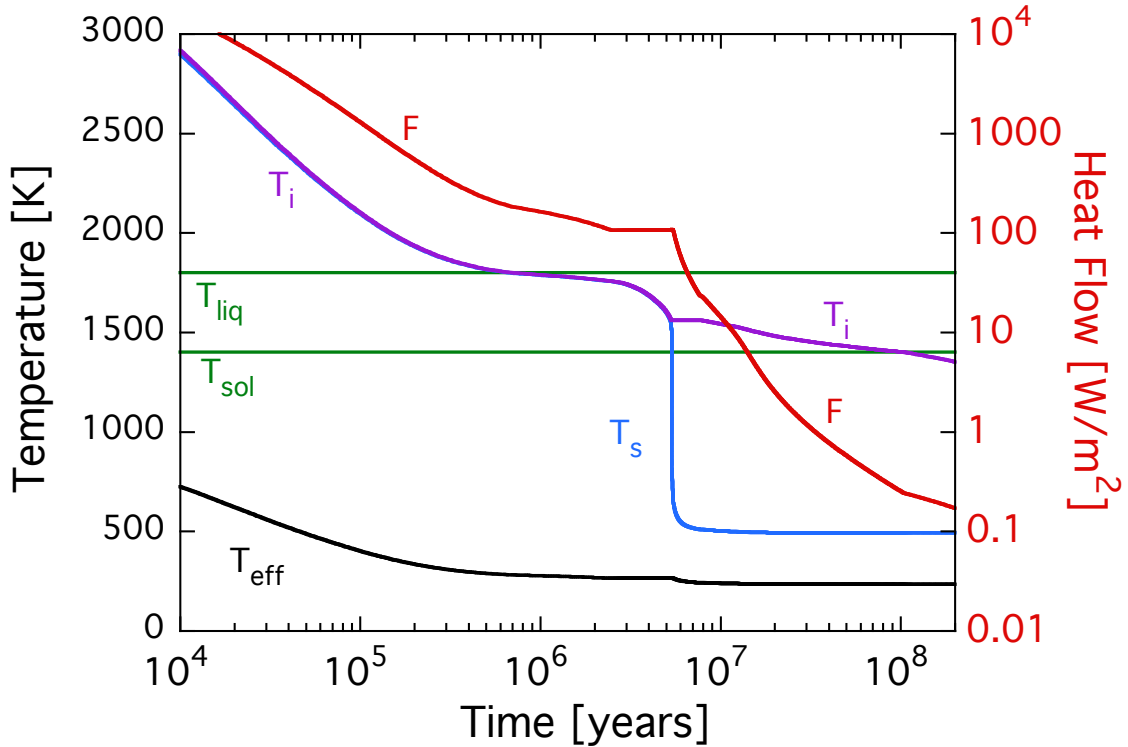


Figure 7: Thermal evolution of the Earth after a high angular momentum Moon-forming impact. Results are shown for 100 bar atmospheres. Excess angular momentum in the Earth-Moon system is removed by the evection resonance, here crudely modeled by holding the Moon at the resonance distance until the angular momentum has been reduced to modern levels. This captures the spirit if not the details of Čuk and Stewart’s model. Compare to Figure 3.

Figure 7 shows thermal evolution of the Earth after a Moon-forming impact. For Earth, the liquid magma ocean phase is prolonged to ~ 6 Myr by the added heat released by tidal dissipation but otherwise resembles the angular momentum conserving case seen in Figure 3 above.

The evolution of Q_{\oplus} in the Earth is the topic of Figure 8, the analog to Figure 5 for a high angular momentum Moon-forming impact. Figure 9 shows lunar recession velocities for the middle case from Figure 8.

In general, tides in the Earth increase the eccentricity of the lunar orbit while

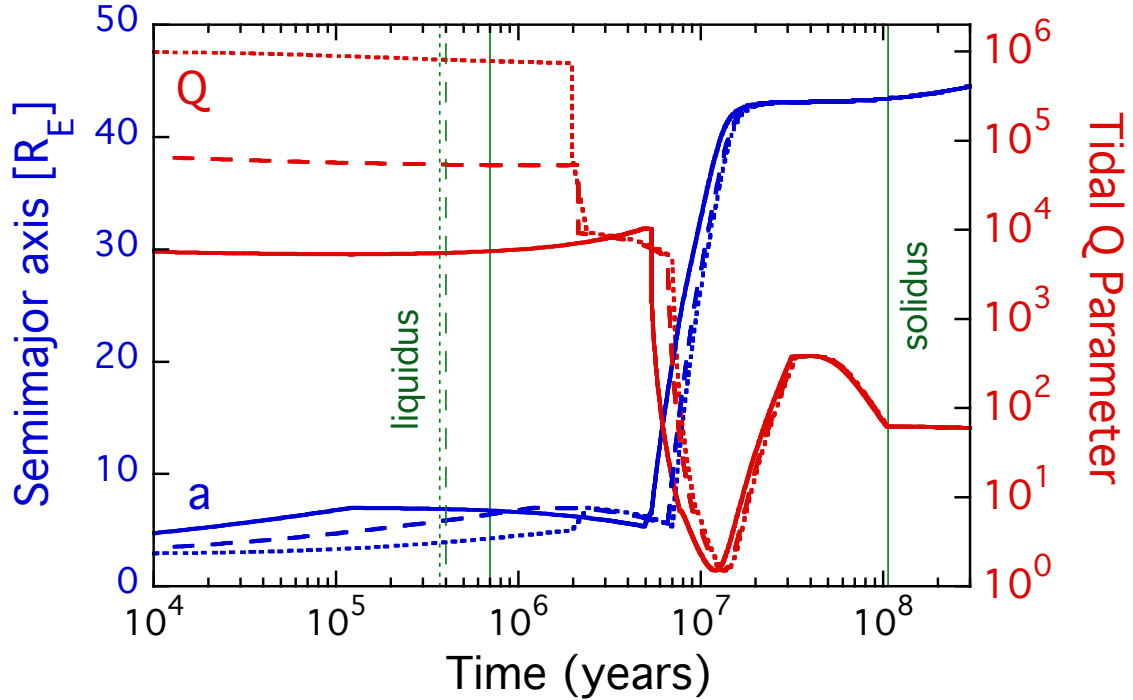


Figure 8: Evolution of lunar distance a and Earth’s Q_{\oplus} after high angular momentum Moon-forming impacts. Three cases are shown that correspond to different upper bounds on Q_{\oplus} in the fully molten Earth. All cases assume the 100 bar BSE-equilibrated atmosphere. Results can be compared to Figure 5 for constant angular momentum.

tides in the Moon decrease the eccentricity of the lunar orbit (Goldreich and Soter, 1966). Recent discussions of lunar orbital evolution have parameterized this struggle as an A factor (Mignard, 1980; Touma and Wisdom, 1998; Ćuk and Stewart, 2012),

$$A \equiv \frac{M_{\oplus}^2 R_{\zeta}^5 k_{2\zeta} Q_{\oplus}}{M_{\zeta}^2 R_{\oplus}^5 Q_{\zeta} k_{2\oplus}} \equiv \frac{\rho_{\oplus}^2 R_{\oplus} k_{2\zeta} Q_{\zeta}}{\rho_{\zeta}^2 R_{\zeta} Q_{\zeta} k_{2\oplus}} \approx 10 \frac{k_{2\zeta} Q_{\zeta}}{Q_{\zeta} k_{2\oplus}}, \quad (32)$$

that quantifies the relative importance of tidal dissipation in the Moon to tidal dissipation in the Earth³ Today $k_{2\zeta} = 0.02$ and $k_{2\oplus} = 0.3$ (Kaula, 1968), which results in $A \approx 0.5$ (with $Q_{\oplus} = 15$). When $A \gg 1$, dissipation is relatively strong in

³The power “5” is incorrectly written “3” in Touma and Wisdom (1998) and Touma (2000).

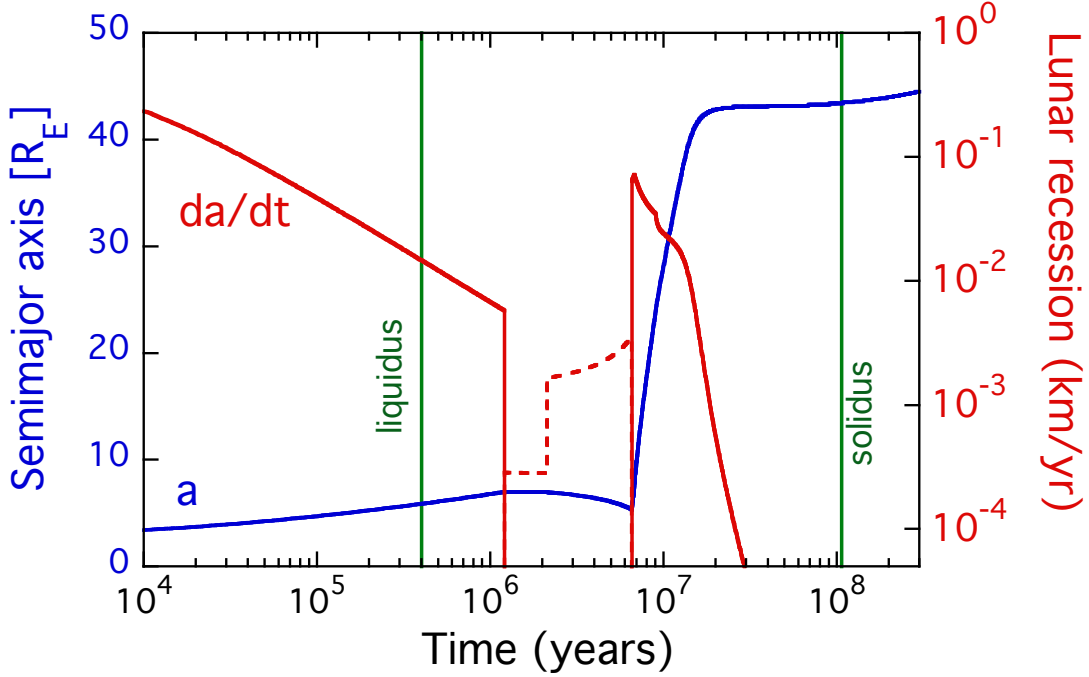


Figure 9: Lunar recession velocities for a high angular momentum Moon-forming impact. The case shown is the middle one from Figure 8. In resonance the Moon approaches the Earth ($da/dt < 0$ indicated by dotted curve). Earth encounters the evection resonance before it begins to solidify. Recession rates are low enough that resonance capture is certain. Details in the structure of da/dt reflect changes in the mantle’s rheological properties as it cools.

the Moon, so that the orbit is circularized. This is expected at early times when Earth is fully molten and Q_{\oplus} is very high, while the Moon has little or no atmosphere and thus quickly cools to a highly dissipative state with Q_{ζ} in the range of 1 to 10. On the other hand, when $A \ll 1$, dissipation in Earth is more important than dissipation in the Moon, so that tides raise the eccentricity of the lunar orbit. This is the case at later times when Earth’s mantle is freezing and $Q_{\oplus} \ll 10$.

All models that we have looked at, with or without resonance capture over a wide range of atmospheres and planetary albedos, predict (apart from an initial transient) the same evolution of A as a function of a (Figure 10; A assumes current lunar parameters of $k_{2\zeta} = 0.02$ and $Q_{\zeta} = 20$). The constancy of $A(a)$ (i.e., of $Q_{\oplus}(a)$,

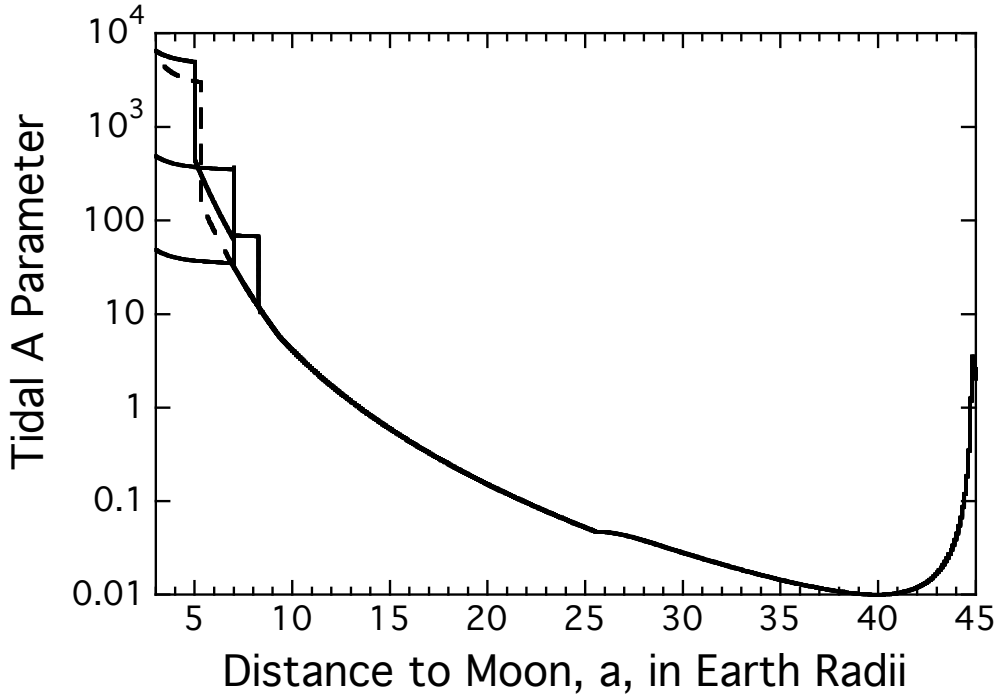


Figure 10: Evolution of the A factor that parameterizes the relative efficiency of tidal dissipation in the Moon to tidal dissipation in the Earth (Eq 32). Lunar parameters $k_{2\zeta} = 0.02$ and $Q_{\zeta} = 20$ are held fixed. Several cases are shown: the conventional case from Fig. 5 (dashed line), the three “evection” cases from 8, and another with a 1000 bar atmosphere (solid lines). Differences at the beginning stem from different assumptions about Q_{\oplus} in the fully molten Earth. Otherwise the course of $A(a)$ is the same in all our models. In all cases the best prospects for growing a lunar eccentricity is with $A \ll 1$, when the distance to the Moon was between 20 and 40 R_{\oplus} .

as $k_{2\oplus}$ does not stray from 1.5 until late) implies that the tidal evolution of $Q_{\oplus}(a)$ is determined by a general principle, probably conservation of energy, rather than by details of our model.

A second key point made in Figure 10 is that, in all cases, $A \gg 1$ when the Moon encounters the evective resonance. In the class of models being considered here, there appears to be no way for tidal evolution to be both slow enough to hold the Moon within $a < 7R_{\oplus}$ yet simultaneously to be highly dissipative (low Q_{\oplus}). The reason for this is that small values of Q_{\oplus} cause fast tidal evolution, quickly raising a

above $15R_{\oplus}$. Thus the Moon could not acquire much eccentricity while in the evection resonance.

A third point made in Figure 10 is that, in all cases, $A \ll 1$ when $20R_{\oplus} < a < 40R_{\oplus}$. In this phase of lunar orbital evolution dissipation in the Earth would have been much more important than dissipation in the Moon, so that tides raised in the Earth by the Moon would have raised the eccentricity of the lunar orbit. How big e can grow is unclear. Touma and Wisdom (1998) found that $e = 0.5$ is achievable in the evection resonance. Presumably tidal flexure in the Moon caused by a highly eccentric orbit would at some point trigger considerable tidal melting within the Moon and a consequent drop of Q_{ζ} . Later still, after the Earth has mostly solidified, A must rise again and most of any remaining eccentricity is taken out of the Moon's orbit.

How a late episode of lunar eccentricity might be twisted into today's lunar inclination is another puzzle beyond the scope of this study. Touma (2000) mentions a secular resonance for growing inclination when the Moon was at $28R_{\oplus}$ if $e > 0.6$, but the mechanism is not otherwise described and we can say no more. We do note that, in general, prospects for giving the Moon an inclination are probably best when the Moon's orbit was neither wholly under the Sun's influence nor the Earth's influence, which roughly corresponds to $15R_{\oplus} < a < 30R_{\oplus}$. During this interval the Laplace plane coincides with neither the ecliptic nor Earth's equator which, if nothing else, creates an opportunity for helpful accidents (Ward, 1981).

4. Conclusions

The greenhouse effect of a thick water-rich atmosphere slows the rate that a planet cools after a giant impact. Here we show that for water-rich atmospheres, the difference between the runaway greenhouse limit of $\sim 280 \text{ W/m}^2$ and absorbed sunlight (which for the faint young Sun and a planetary albedo of 0.3 is $\sim 170 \text{ W/m}^2$) sets an upper bound of $\sim 110 \text{ W/m}^2$ on how quickly the Earth can cool. This in turn sets a 10^6 year timescale for a magma surface after an impact on the

scale of the event that formed the Moon.

Tidal heating is a major term in the early Earth’s energy budget. Tidal heating occurs mostly in mantle materials that are just beginning to freeze, which frustrates freezing. The atmosphere’s control over the planet’s cooling rate sets up a negative feedback between viscosity-dependent tidal heating and the temperature-dependent viscosity of the magma ocean. While this feedback holds, the rate that the Moon’s orbit evolves is limited by the modest radiative cooling rate of Earth’s atmosphere, which in effect tethers the Moon to the Earth. Consequently the Moon’s orbit evolves orders of magnitude more slowly than in conventional models that describe tidal evolution through fixed values of Q (Touma and Wisdom, 1998; Čuk and Stewart, 2012). The slow tidal evolution ensures that the evolving Earth-Moon system will be captured by the strong evection resonance, but in our models the resonance encounter always occurs when tidal dissipation is more efficient in the Moon than in the Earth, which suggests that capture by the evection resonance is unlikely to generate much eccentricity in the lunar orbit. Whether significant angular momentum can be extracted from the Earth-Moon system by cumulative solar torques from a low eccentricity lunar orbit is a question beyond the scope of this research, but the answer to this question would have implications for Čuk and Stewart (2012)’s inventive hypothesis.

Slow orbital evolution also promotes capture by other, weaker, higher order resonances (Touma and Wisdom, 1998; Touma, 2000). Resonance capture by one or more of these resonances may have play a key role in the orbital evolution of the Earth-Moon system, a possibility raised but not elaborated upon by Touma and Wisdom (1998). Tidal dissipation in the Earth is most efficient at later times when the Earth’s mantle has cooled enough to develop significant viscosity. In all our models, tidal dissipation is most efficient in the Earth when the Moon is between $20R_{\oplus}$ and $40R_{\oplus}$. During this interval it is likely that the Moon’s eccentricity grew considerably. The upper limit on eccentricity may be set by vigorous tidal heating in the Moon — once the Moon melts, tidal dissipation in the Earth and the Moon will

be more comparable. We speculate that this period of high eccentricity set the table for some other process, perhaps capture by an otherwise unremarkable, little-noted resonance, that exploited its opportunity by leaving its mark on the inclination of the Moon.

Acknowledgments

The authors thank the NASA Planetary Atmospheres Program for support of this work.

References

References

- Abe, Y., 1997. Thermal and chemical evolution of the terrestrial magma ocean. *Phys. Earth Planet. Int.* 100, 2739.
- Abe, Y., Matsui, T., 1988. Evolution of an impact-generated H₂O-CO₂ atmosphere and formation of a hot proto-ocean on Earth. *J. Atmos. Sci.* 45, 3081–3101.
- Benz, W., Slattery, W.L., Cameron, A.G.W., 1986. The origin of the moon and the single-impact hypothesis. *Icarus* 66, 515-535.
- Canup, R.M., 2004. Dynamics of Lunar Formation. *Ann. Rev. Earth Planet. Sci.* 42, 441–475.
- Canup, R.M., 2012. Forming a Moon with an Earth-like Composition via a Giant Impact. *Science* 338, 1052-1055.
- Canup, R.M., Righter, K., (Eds.), 2000. *Origin of Earth and Moon*. University of Arizona Press, Tucson.
- Ćuk, M., Stewart, S., 2012. Making the Moon from a Fast-Spinning Earth: A Giant Impact Followed by Resonant Despinning. *Science* 338, 1047-1051.

- Elkins-Tanton, L., 2008. Linked magma ocean solidification and atmospheric growth for Earth and Mars. *Earth Planet. Sci. Lett.* 271, 181191.
- Elkins-Tanton, L., 2012. Magma Oceans in the Inner Solar System. *Ann. Rev. Earth Planet. Sci.* 40, 113-139.
- Fegley, B., Schaefer, L., 2013. Chemistry of the Earth's Earliest Atmosphere. In: *Treatise on Geochemistry*. Vol. 13. Elsevier. eprint arXiv:1210.0270.
- Garrick-Bethell, I., Nimmo, W.H.F., Wieczorek, M., 2010. Structure and Formation of the Lunar Farside Highlands. *Science* 330, 949.
- Genda H., Abe Y., 2000. Escape from an Impact-Generated Proto-Moon Disk. ISAS 2000.
- Goldblatt, C., Zahnle, K.J., Crisp, D., Robinson, T., 2013. *Nature Geosci.*
- Goldreich, P., 1966. History of the lunar orbit. *Rev. Geophys.* 4, 411-439.
- Goldreich, P., Soter, S., 1966. Q in the Solar System. *Icarus* 5, 375–389.
- Hamano, K., Abe, Y., Genda, H., 2013. Emergence of two types of terrestrial planet on solidification of magma ocean. *Nature* 497, 607610.
- Hartmann, W.K., Phillips, R.J., Taylor, G.J. (Eds.), 1986. *Origin of the Moon*. Lunar and Planetary Institute, Houston.
- Hellier, C., and 22 others, 2009. An orbital period of 0.94 days for the hot-Jupiter planet WASP-18b. *Nature* 460, 1098-1100.
- Ida, S., Canup, R., Stewart, G., 1997. *Nature*, 389, 353-357.
- Kaula, W.M., 1968. *An Introduction to Planetary Physics: The Terrestrial Planets*. Wiley.
- Kopperapu, R., Ramirez, R., Kasting, J.F., Robinson, T., 2013. *Astrophys. J.*

- Lainey, V., Arlot, J.-E., Karatekin, O., Van Hoolst, T., 2009. Strong tidal dissipation in Io and Jupiter from astrometric observations. *Nature* 459, 957-959.
- Lainey, V., and 10 others, 2012. Strong tidal dissipation in Saturn and constraints on Enceladus's thermal state from astrometry. *Astrophys. J.* 752, 14 (19pp).
- Lamb, H., 1932. *Hydrodynamics*. Dover.
- Lambeck, K., 1980. *Earth's Variable Rotation*. Wiley.
- Lebrun, T., Massol, H., Chassefiere, E., Davaille, A., Marcq, E, Sarda, P., Leblanc, F., Brandeis, G., 2013. Thermal evolution of an early magma ocean in interaction with the atmosphere: conditions for the condensation of a water ocean. EGU2013-4653.
- Lupu, R., Marley, M., Schaefer, L., Fegley, B., Morley, C., Cahoy, K., Freedman, R., Fortney, J.J., Zahnle, K.J., 2014. The atmospheres of Earth-like planets after giant impact events. *Astrophys. J.* 784: 27 (19pp).
- Makarov, V. V., Efroimsky, M., 2014. Tidal dissipation in a homogeneous spherical body. II. Three examples: Io, Mercury, and Kepler-10 b. *Astrophys. J.* 795: 7.
- Matsui, T., Abe, Y., 1986. Impact-induced atmosphere and oceans on Earth and Venus. *Nature* 322, 526-528.
- Meibom, S., Mathieu, R.D., 2005. A robust measure of tidal circularization in coeval binary populations: the solar-type spectroscopic binary population in the open cluster M35. *Astrophys. J.* 620, 970-983.
- Mignard, F., 1980. The evolution of the lunar orbit revisited, II. *Moon and Planets* 23, 185-201.
- Moore, W.B., 2003. Tidal heating and convection in Io. *J. Geophys. Res.* 108, 5096, doi:10.1029/2002JE001943.

- Pahlevan, K., Stevenson, D.J., 2007. Equilibration in the aftermath of the lunar-forming giant impact. *Earth Planet. Sci. Lett.* 262, 438–449.
- Reufer, A., Meier, M.M.M., Benz, W., Wieler, R., 2012. A hit-and-run giant impact scenario. *Icarus* 221, 296299.
- Salmon, J., Canup, R.M. 2012. Lunar accretion from a Roche-Interior fluid disk. *Astrophys. J.* 760, 83 (18pp).
- Schaefer, L., Fegley, B., 2010. Chemistry of atmospheres formed during accretion of the Earth and other terrestrial planets. *Icarus* 208, 438-448.
- Schaefer, L., Lodders, K., Fegley, B., 2012. Vaporization of the Earth: Application to Exoplanet Atmospheres. *Astrophys. J.* 755, article id. 41, 16 pp.
- Sleep N.H., Zahnle, K.J., Neuhoff, P.S., 2001. Initiation of clement surface conditions on the earliest Earth. *Proc. Nat. Acad. Sci.* 98, 3666-3672.
- Sleep N.H., Zahnle, K.J., Lupu, R.S., 2014. Terrestrial aftermath of the Moon-forming impact. *Phil. Trans. Roy. Soc. A* 372, 20130172.
- Solomatov, V.S., 2009. Magma oceans and primordial mantle differentiation. Chapter 3. in: Stevenson, D.J. (Ed.), *Treatise on Geophysics Vol. 9. Evolution of the Earth.* Elsevier, pp. 91-120.
- Stevenson, D.J., 1987. Origin of the Moon – the Collision Hypothesis. *Ann. Rev. Earth Planet. Sci.* 15, 271–315.
- Thompson, C., Stevenson, D.J., 1988. Gravitational instability in two-phase disks and the origin of the Moon. *Astrophys. J.* 333, 452-481.
- Tonks, W.B., Melosh, H.J., 1993. Magma ocean formation due to giant impacts. *J. Geophys. Res.* 98, 5319-5333 DOI: 10.1029/92JE02726.

- Touma, J., Wisdom, J., 1998. Resonances in the early evolution of the Earth-Moon system. *Astron. J.* 115, 1653-1663.
- Touma, J., 2000. The phase space adventure of the Earth and Moon. in: Canup R.M., Righter, K., (Eds.), *Origin of the Earth and Moon*. Tucson: University of Arizona Press., pp. 165-178.
- Ward, W.R. 1981. Orbital inclination of Iapetus and the rotation of the Laplacian plane. *Icarus* 46, 97-107.
- Ward, W.R., Canup, R. 2000. Origin of the Moon's orbital inclination from resonant disk interactions. *Nature* 403, 741-743
- Zahnle, K.J., Kasting, J.F., Pollack, J.B., 1988. Evolution of a steam atmosphere during Earth's accretion. *Icarus* 74, 62-97.
- Zahnle, K.J, Arndt, N., Cockell, C., Halliday, A.N., Nisbet, E.G., Selsis, F., Sleep, N.H., 2006. Emergence of a habitable planet. *Space Sci. Rev.* 129, 35-78.
- Zhang, J., Dauphas, N., Davis, A.M., Leya, I., Fedkin, A., 2012. The proto-Earth as a significant source of lunar material. *Nature Geoscience*, DOI: 10.1038/NNGEO1429.